

Numerical validation of the incremental launching method of a steel bridge through a small scale experimental study

R. Chacón*, N. Uribe*, S. Oller**

*Construction Engineering Department

**International Centre for Numerical Methods in Engineering (CIMNE)

Universitat Politècnica de Catalunya. Barcelona Tech

Submitted for copyediting and typesetting in

Experimental Techniques

Abstract

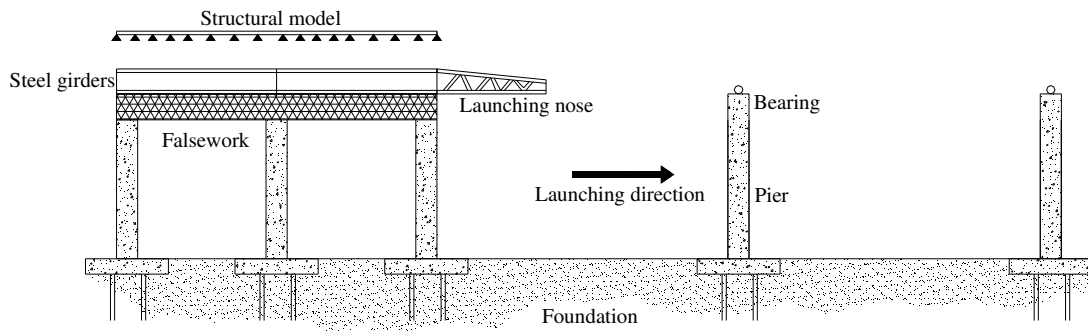
This paper presents an experimental and a numerical study of an incremental launching process of a steel bridge. The former is deployed in a scale-reduced laboratory whereas the latter, is performed using the finite element method. The numerical simulation is based upon realistic transient boundary conditions and accurately reproduces the elastic response of the steel bridge during launching. This numerical approach is validated experimentally with the scale-reduced test performed at the laboratory. The properly validated numerical model is subsequently systematically employed as a simulation tool of the process. The proposed simulation protocol might be useful for design and monitoring purposes of steel bridges to be launched. Results concerning strains, stresses and displacements might be inferred from the model and thus compared to field measurements obtained in situ. The conditions presented at the end of the paper are potentially useful for researchers and practice engineers alike.

Keywords: Incremental launching method. Steel bridges. Bridge monitoring

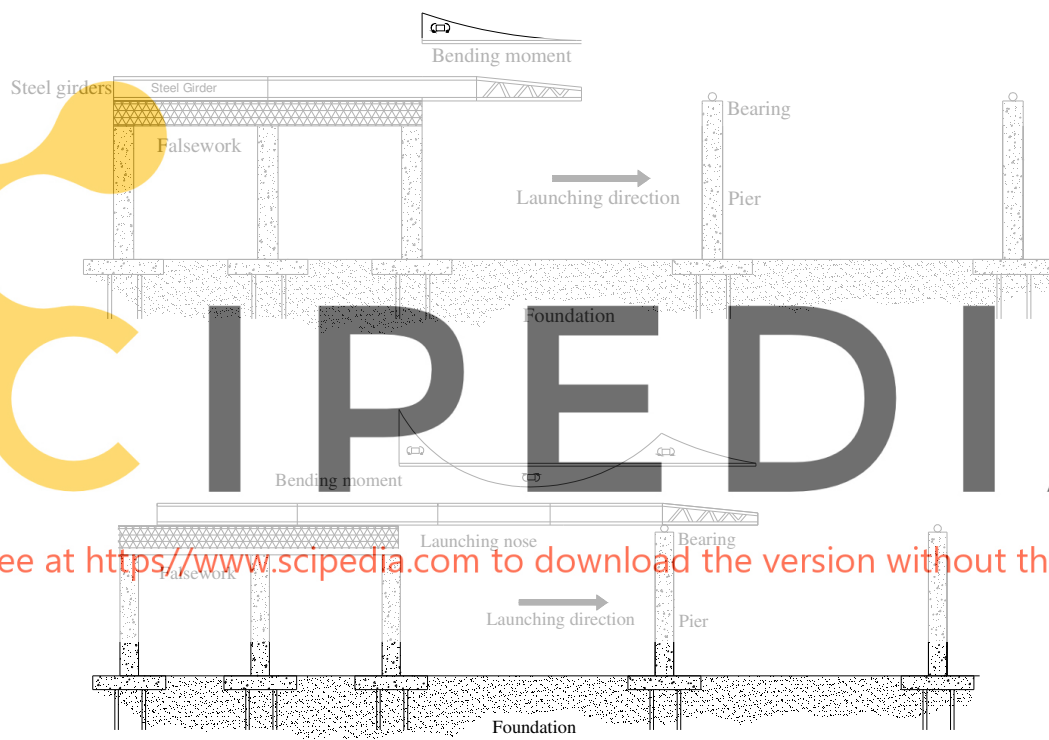
1. Introduction

The incremental launching method (ILM) has gained increasing popularity in last decades as a construction method of short- to large- multi-spanned steel and/or concrete bridges [1]. ILM consists of assembling the superstructure on one side of the obstacle to be crossed and then pushed longitudinally (or “launched”) into its final position. Generally, steel bridges are completely assembled prior to launching operations. In concrete bridges, however, the launching is typically performed in a series of increments so that additional sections can be added to the rear of the superstructure unit prior to subsequent launches. The ILM may offer advantages over conventional construction techniques when the construction takes place in environmentally protected areas, or areas at which minimal disturbances to surroundings are needed, thus providing a more concentrated work area for the superstructure assembly. Safety concerns might also be reduced if ILM is employed [1-3]. During the launching operation, the bridge superstructure is supported by a series of rollers or sliding bearings. The thrust required to launch

or hollow-core strand jacks [1]. Fig. 1 shows a lateral schematic view of an incrementally launched steel girder. It is worth pointing out the continuous change of the static conditions. In Fig. 1, the varying bending moment diagrams are qualitatively included for illustration.

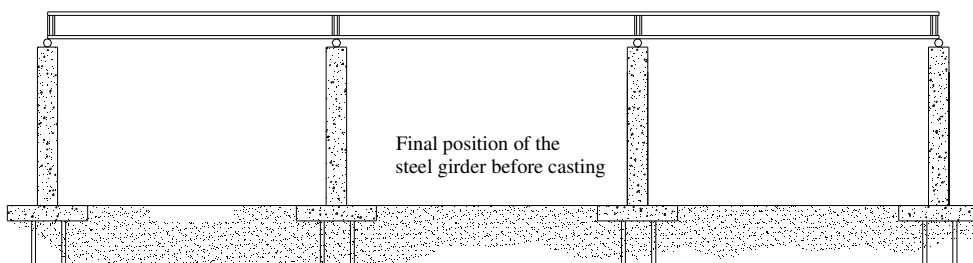


43



44

Register for free at <https://www.scipedia.com> to download the version without the watermark



45

46

47

48

Figure 1. Incremental launching method of a steel bridge.

ILM has reportedly been used for the first time in Venezuela during the sixties for a bridge over the Caroni River [3]. Ever since that, hundreds of steel and/or concrete bridges have been built worldwide using the ILM. A close inspection of the vast database given in [1] gives a worth mentioning twofold observation: Europe has a vaster tradition of systematic usage of ILM than the U.S.A and the vast majority of launched bridges are made of post-tensioned concrete.

Admittedly, according to [1], there has historically been a knowledge gap between designers, contractors and bridge owners when it comes to the systematic usage of ILM. ILM requires a considerable amount of analysis and design expertise and specialized construction equipment. A detailed structural analysis of all construction phases is compulsory. It is necessary to take into account the continuous change of the structural scheme due to the transient conditions of the supports. Internal as well as external forces acting on the rollers might considerably change throughout the process. The stress state at the final phase of the bridge girders might differ

considerably (in magnitude and sign) from the stress states that have been carried out during launching. Furthermore, it is a matter of fact that the launching of bridges made of concrete

requires a different set of solutions than those required for purely metallic bridges. For the former, the design of the post-tensioning system must consider not only dead load stresses, but also the considerable stress reversals that occur during launching. For the latter, there are a number of issues related to large concentrated forces applied to the girder (namely, patch loading) as well as to the torsional stiffness of an open section, such as an I-girder, that must be carefully addressed by the designer in order to avoid an undesired instability-related collapse.

SCIPEDIA

Register for free at <https://www.scipedia.com> to download the version without the watermark

This paper presents numerical and scale-reduced experimental reproductions of a steel bridge whose construction process is the ILM. The numerical reproduction is performed using a FE-based commercial Software that is properly validated with a scale-reduced model deployed at the Laboratory of the Chair of Strength of Materials-Technical University of Catalonia (UPC). The numerical model is based upon a contact formulation and allows to reproduce the continuous change of the boundary conditions of the launched girders. The results provided by the numerical model include stresses, strains, displacements and support reactions that might be compared *in situ* to field measurements during the whole process. These comparisons might be of the utmost importance for control and monitoring engineers. Consequently, the results presented at the end of the paper are aimed at showing relevant information for designers, contractors and bridge owners alike.

2. State of the art

The ILM has been developed thoroughly during the last decades in several works and papers available in the literature that address this topic with a broad perspective [1-6]. More specific papers concerning particular topics of the method have continuously been published. Rosignoli has focused his research to the design of the bridges, the launching noses and the rolling devices [7-11] whereas Granath has pointed out the structural response of particular elements of the steel bridges that are exposed to concentrated loads of considerable magnitude [12-14]. On the other hand, several publications related to bridges constructed using the ILM are available [1] [15-17].

Publications related to the numerical simulation of incrementally launched steel bridges are, however, rather scarce. Marzouk et al [18] performed several applications of computer

SCIPEDIA

Register for free at <https://www.scipedia.com> to download the version without the watermark

simulations of incrementally launched bridges. Their main purpose was to improve the design of the bridge to be launched by developing optimization algorithms. Ronggiao and Shao [19] developed a new beam finite element suitable to reproduce the continuous changes in the support conditions when a superstructure is constructed using the ILM.

Moreover, it has been of the utmost importance to monitor steel bridges while being launched.

During the launching phase, the process is usually monitored via reaction at supports/rollers or via displacement using topography equipment [2]. These controls are discretely measured in

regions that are anticipated to be somewhat critical. Recently, Chacón et al. [20] performed a

research work aimed at monitoring the strain levels of the steel girders with wireless sensors. The

results have been useful at research levels showing that wireless technology might be

considerably useful during such construction process. Other researchers have already

implemented monitoring deployments over incrementally launched steel bridges with various

levels of accuracy and/or amount of collected data [21-23]. Publications related to computer-aid

design and visualization of launched bridges are also available [24].

Register for free at <https://www.scipedia.com> to download the version without the watermark

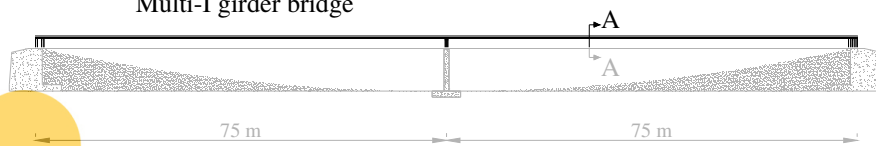
3. Scale-reduced experimental simulation of the ILM

3.1 General

An experimental reproduction of an incremental launching procedure of a steel bridge was deployed at the Laboratory of the Chair of Strength of Materials-Technical University of Catalonia (UPC). The objective was to reproduce a launching procedure of a medium- multi-spanned bridge assembled with steel I-girders. This prototype is a standard design routinely employed in road bridges [25]. The chosen geometry for the reproduction is a laterally-restrained, steel multi-I-girder whose final configuration is a continuous and symmetric two-

spanned multi I-girder beam with a total length of 150 meters and a single central pier (Fig.2). The generic cross-section dimensions of the analyzed girder are also included. For the sake of simplicity, only one girder (bolded in Fig. 2) is considered in the analysis. The other girders are displayed in dashed lines only for illustration purposes.

Cross-Section A-A
Multi-I girder bridge



Cross-Section A-A

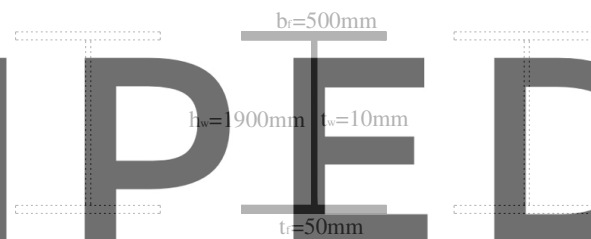


Figure 2. Prototype longitudinal and transversal view.

The depicted prototype was scale-reduced for a proper adaptation to the laboratory facilities. The reduced model was inferred from a thorough comparison between the prototype geometry, the laboratory facilities and by applying the PI-Buckingham theorem [26-27]. The theorem roughly states that a physically meaningful equation (in this case, structurally meaningful) involving a certain number n of parameters is equivalent to an equation involving a set of $p = n - k$ dimensionless parameters constructed from the original variable (being k the number of independent fundamental physical quantities).

133 Table 1 shows the considered "n" structural parameters (including numerical values) whereas
 134 Table 2 shows the "p" chosen dimensionless groups. Thus, the prototype was structurally scale-
 135 reduced to the experimental model

Symbol	Description	SI units	Prototype	Scale reduced model
E	Elasticity modulus	N/mm ²	210000	210000
ν	Poisson's ratio	-	0,3	0,3
L	Span length	m	75	1
Q	Self-weight	kN/m	5,42	$1,88 \cdot 10^{-2}$
M	Bending moment	kN-m	15,23	$9,42 \cdot 10^{-3}$
σ	Stress	N/mm ²	286	58,9
ϵ	Strain	-	$1,43 \cdot 10^{-3}$	$2,94 \cdot 10^{-4}$
δ	Vertical displacement	mm	2010	37
ϕ	Rotations at supports	rad	$3,58 \cdot 10^{-2}$	$4,91 \cdot 10^{-2}$
W	Section modulus	mm ³	53257,5	160
F	Forces (Reactions)	kN	406,24	$1,88 \cdot 10^{-2}$

Register for free at <https://www.scipedia.com> to download the version without the watermark

Table 1. Structural parameters.

Dimensionless Group	Similarity	Structural parameters	Dimensionless ratios	Scale factor
1	$\pi_1 = \pi'_1$	$\frac{F}{E \cdot l^2} = \frac{F'}{E' \cdot l'^2}$	$\lambda_f = \lambda_l^2$	$\left(\frac{1}{75}\right)^2$
2	$\pi_2 = \pi'_2$	$v = v'$	$\lambda_v = 1$	1
3	$\pi_3 = \pi'_3$	$\frac{q}{E \cdot L} = \frac{q'}{E' \cdot L'}$	$\lambda_l = \lambda_q$	$\left(\frac{1}{75}\right)$
4	$\pi_3 = \pi'_3$	$\frac{M}{p \cdot l} = \frac{M'}{p' \cdot l'}$	$\lambda_M = \lambda_l$	$\left(\frac{1}{75}\right)$
5	$\pi_5 = \pi'_5$	$\sigma = \sigma'$	$\lambda_\sigma = 1$	1
6	$\pi_6 = \pi'_6$	$\varepsilon = \varepsilon'$	$\lambda_\varepsilon = 1$	1
7	$\pi_7 = \pi'_7$	$\frac{\delta}{l} = \frac{\delta'}{l'}$	$\lambda_\delta = \lambda_l$	$\frac{1}{75}$
8	$\pi_8 = \pi'_8$	$\phi = \phi'$	$\lambda_\phi = 1$	1
9	$\pi_9 = \pi'_9$	$\frac{l^3}{w} = \frac{l'^3}{w'}$	$\lambda_w = \lambda_l^3$	$\left(\frac{1}{75}\right)^3$

Register for free at <https://www.scipedia.com> to download the version without the watermark

145 A close inspection of Tables 1 and 2 leads to pinpoint a threefold observation:

- 146
- Dimensionless groups 7 and 9 define the scale-reduced model geometry, that is to say,
- 147 the ratio between vertical displacement and the span length.
- 148
- The self-weight is not considered in the structural variables as a mass force. The
- 149 prototype and the scale-reduced model are made of the same material (steel). Therefore,
- 150 both have identical values of density, Young's modulus and Poisson's ratio.
- 151

- 152
- 153 • Strains, stresses, and Poisson's ratio (groups 2,5 and 6) remained unaltered in the
- 154 reduced model. These magnitudes do not play any role when calculating the scaled
- 155 model geometry. However, from a simplified static analysis of the phenomenon, it was
- 156 inferred and verified that the stresses obtained at any point on the steel plate should not
- 157 exceed the yield point threshold.

158

159 In its final stage, the steel plate was a symmetric two-spanned continuous beam with a total

160 length of 2000 mm and a rectangular 60mm·4mm cross section. This section is chosen for the

161 sake of accomplishing the scale of the inertia (an I-beam would provide a major-axis inertia that

162 would require a longer span). The steel plate was designed with a launching nose with the same

163 cross-section and material. This plate was launched from one support another by means of a

164 roller system designed at the laboratory facilities. The length scale (pointed out in Table 2) was

165 not precisely obtained since the cross-section had to be adapted to the available commercial steel

166 profiles.

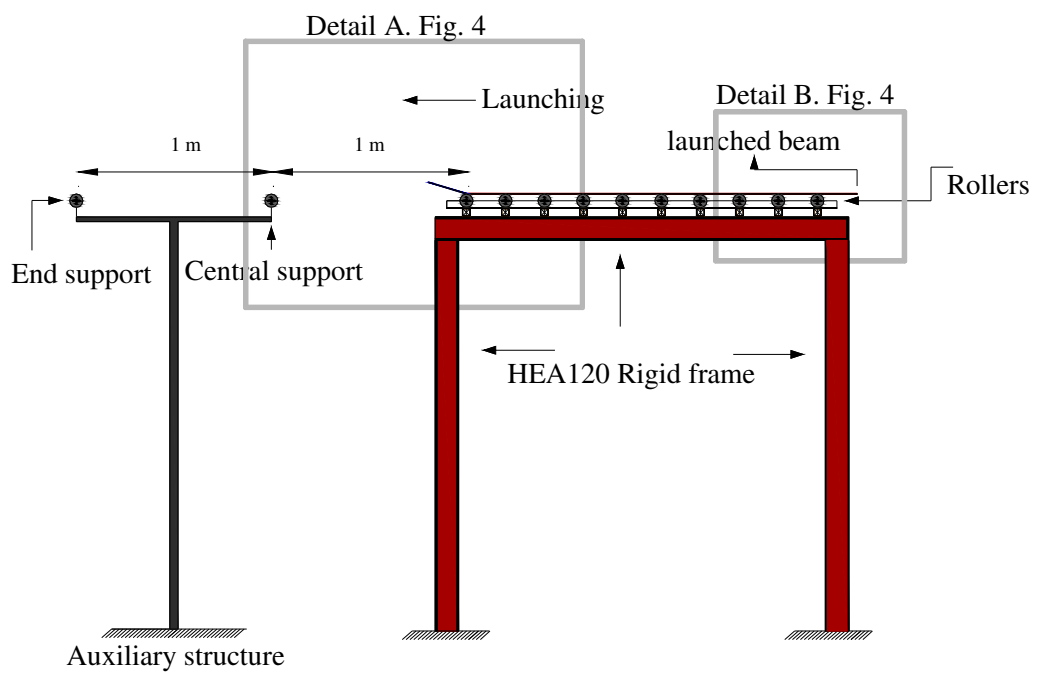
167 Fig. 3 depicts the rolling system, the rigid supports that provided the central pier, the dimensions

168 of the launching nose as well as the end support. Fig. 4 shows details A and B (displayed in Fig.

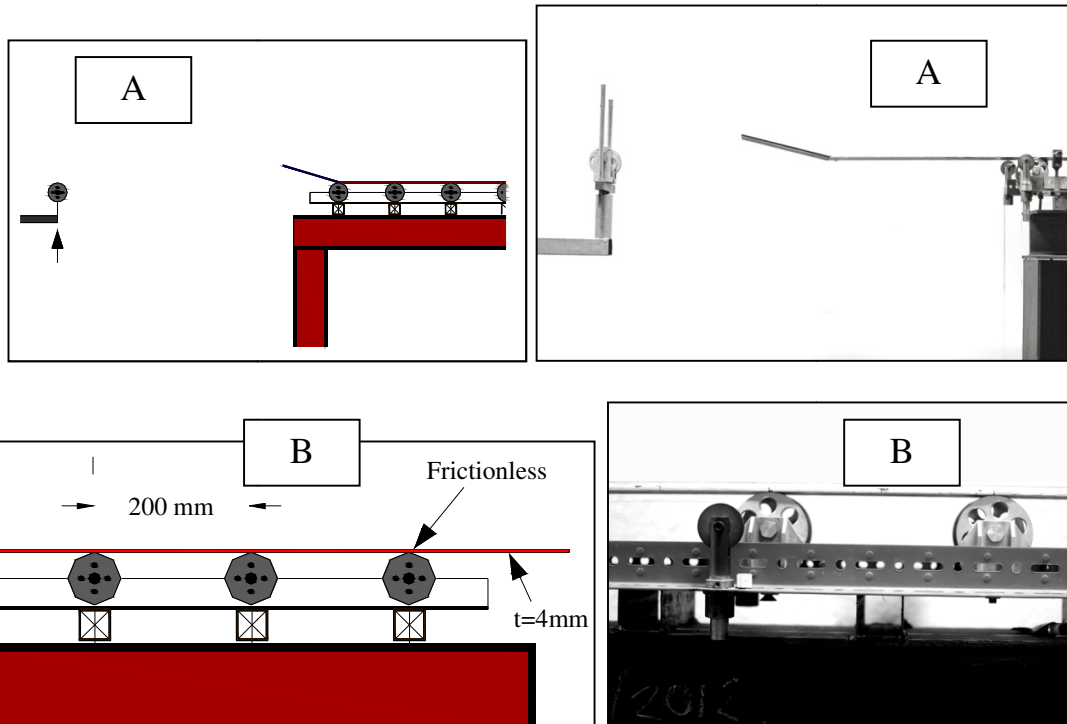
169 3) of the scale-reduced launching procedure. It is worth pointing out the following features:

- 170
- 171 • The rolling system was frictionless.
- 172 • Lateral restraints were added to the system for the sake of avoiding lateral displacements.
- 173 • The launching nose allowed the plate to reposition once the central and/or the end
- 174 supports were approached by the launched steel plate.

- The launching was carried out as a series of increments with halts every 100 mm in order to minimize the potential effect of vibrations (especially in advanced cantilever phases prior to contact with the roller bearings).
- The test was repeated a statistically significant number of times ($n=30$) and the results showed statistical consistency.



• Figure 3. Laboratory test set up.



• Figure 4. Details A and B of the scale-reduced model

3.2 Measurements

Two types of measurements were collected during the launching procedure: strains and displacements at key points of the systems previously anticipated from theoretical calculations. For the former, two strain gauges were bonded (longitudinally and transversely) at the point where the maximum longitudinal stress was expected (precisely at the center of the steel plate, see Fig. 4). The uni-axial gauges (HBM K-RY81-6) were bonded only on the upper fiber of the steel plate to avoid any contact between roller and strain gauge. For the latter, the vertical displacements of key points of the steel plate were collected by means of a photogrammetric procedure using a HD camera. The pictures were digitalized and scaled precisely. Accurate measurements were performed on the digital files. These results were further used to validate a

numerical model. The strain results were collected with a Spider 8 data acquisition system. The signal was processed using the software CATMAN EASY 6.10 [28].

3.3 Experimental results

3.3.1 Strain

Fig. 5 shows the results concerning the strain evolution on the top fiber of the steel plate during incremental procedure. The procedure as well as the plot are divided into five stages for readability:

- Zone A: The steel plate is supported by the rollers system, the measurement equipment was initialized, and the launching system was set up.
- Zone B: The launching procedure starts and the plate behaves like a cantilever with the upper fiber subjected to tensile stresses (positive in the plot). The maximum level of strain collected at this stage was $264\mu\text{m/m}$ before the launching nose reached the central supports. Assuming that the Hooke's law governs the relationship between stresses and strain of the steel plate, the maximum stress recorded at this stage was approximately 54 N/mm^2 .
- Zone C: The launching nose approaches the central support. The structural scheme suddenly changes and sign reversals of the internal forces are observed. During this stage the plate undergoes a sign reversal that ranges from the maximum tensile strain to the maximum compression strain at the top fiber (negative in the plot).

- Zone D: The launching procedure is continuously updated by the transient support conditions and the length of the cantilever which is formed at the second span. The longitudinal strain reaches a value of $264\mu\text{m/m}$ (approximately 58 Mpa of tensile on the top fiber) as it approaches the end support.
- Zone E: The launching nose reaches its final configuration. The steel plate forms a continuous two-spanned beam. It is worth mentioning that at this stage the registered strain level is considerably lower than the strain level recorded during launching. This fact shows the importance of a prior detailed structural analysis that depicts the launching procedure.

It is worth pointing out that as the stepwise nature of the experimentally collected data comes as a result of the elapsed time between successive increments of the experimental incremental launching procedure.

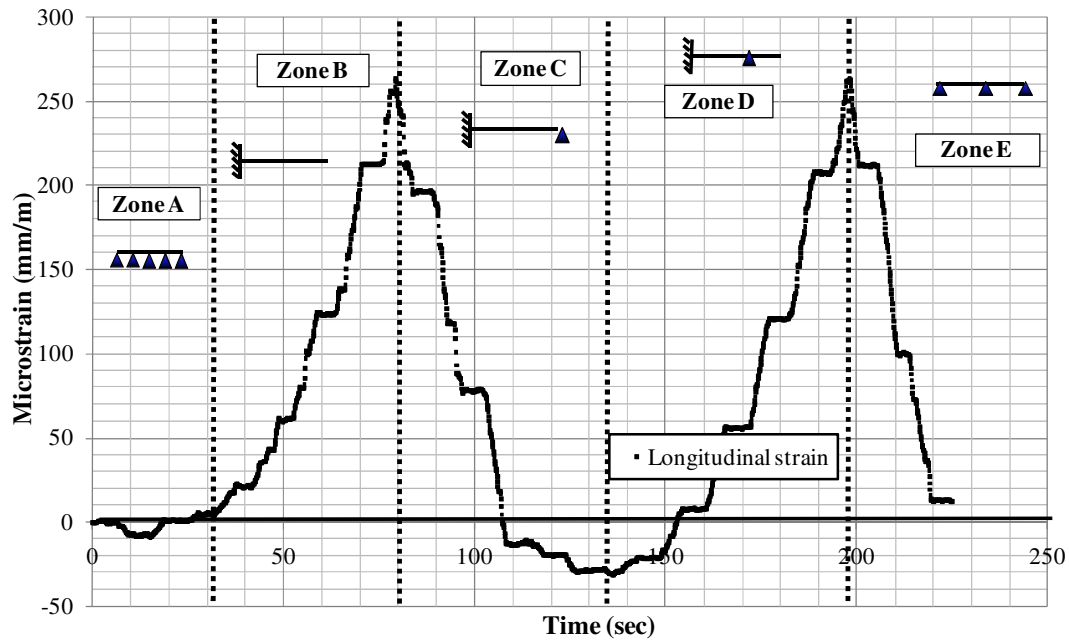


Figure 5. Strain evolution at the upper fiber of the steel plate during the launching.

3.3.2 Vertical displacements

Fig. 6 shows the schematic procedure that has been used for tracking the vertical displacement of the monitored point. The procedure consisted of placing a fixed HD camera that was shot regularly by means of a time-lapse application. The series of pictures were exported and treated with a CAD tool that allowed to measure the location of the monitored point with a high level of accuracy. Fig. 7 shows the tracked vertical displacement at every step of 100 mm. In addition, the theoretical results of the vertical displacement of a similar system (the inclination of the launching nose of such system was disregarded for simplicity) are included within the plot. These theoretical results are based upon a classical Bernoulli beam formulation.

In Fig. 7, it is observable that the maximum deflection was registered during the zone B, at which the plate acts as a cantilever. The maximum measured vertical displacement is 40,5 mm.

At this point, the theoretical value calculated for a cantilever beam using the elasticity theory is 38mm. The difference is attributable to the boundary conditions idealized in theory (fully restrained length of the beam while placed on the roller system) as well as to the simplification of the flat launching nose. The experimental test showed that at maximum cantilever stages, the steel plate is not fully supported by the rollers since some gaps were observed (Fig. 8). Consequently, the experimentally measured deflection was greater than the one anticipated by the theoretical analysis. Further details concerning the description of the experimental results are given in [29].

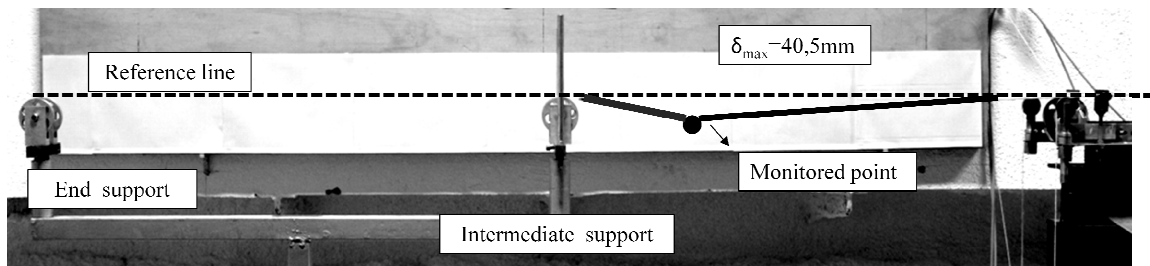


Figure 6. Vertical displacement at monitored point.

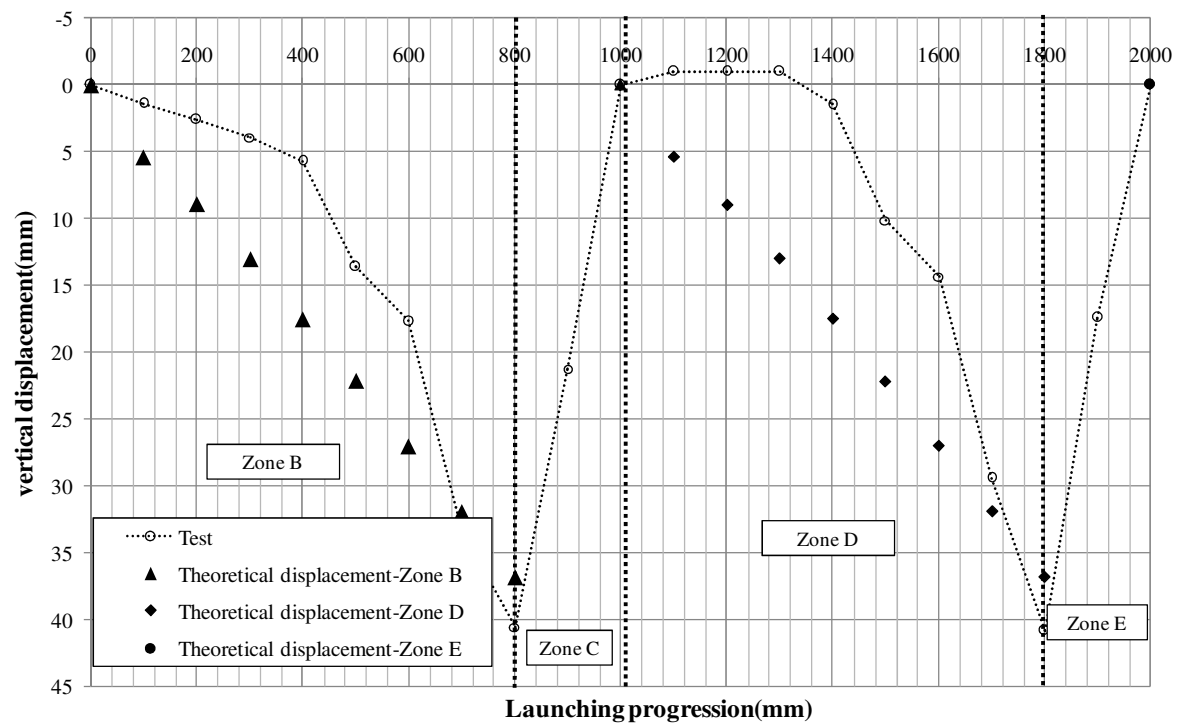


Figure 7. Elastic curve at monitored point.

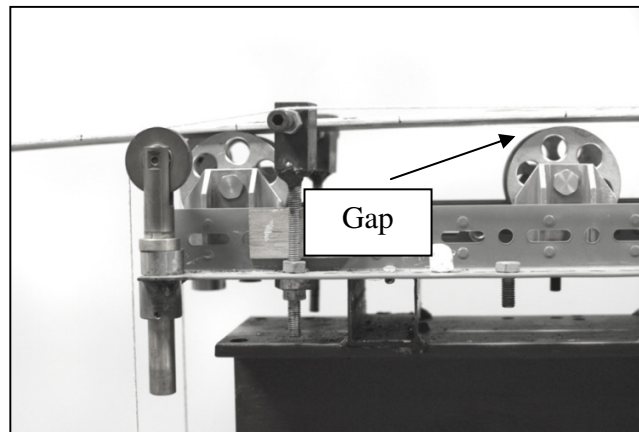


Figure 8. Observable gaps on top of the rollers

3.3.3 Statistical consistency

A total number of 30 tests were performed. Using the non-parametric Kolmogorov-Smirnov test [30] (K-S) for the maximum strain values obtained at the tracked point in Fig. 6, the sample fitted adequately with a normal distribution. Therefore the following statistics: mean, standard deviation and variation coefficient were used to describe the experimental sample (Fig. 9). It is observable that the obtained values of maximum strain were reasonably centered on $267\mu\text{m/m}$

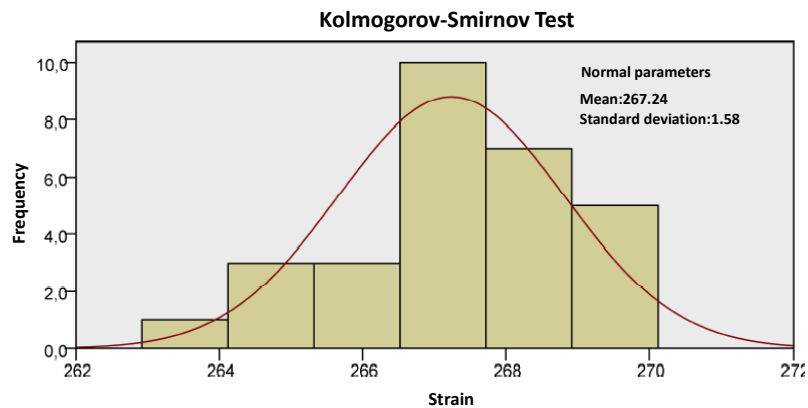


Figure 9. Frequency of the obtained values (maximum recorded microstrain).

4. Numerical reproduction of the scaled-reduced ILM

4.1 Numerical model

A numerical model implemented in the multi-purpose commercial Software Abaqus-Simulia [31] was used as a numerical simulation tool. The numerical model is based upon FEM and is able to reproduce a vast spectrum of physical phenomena. In this particular case, the numerical model was expected to reproduce a multi-body physical problem that involved a mechanical interaction between the steel plate and the support conditions (the rollers). Two features

characterize the modeling of the phenomenon: The geometrical nonlinearity of the problem and the contact-based formulation of the system.

Several approaches for modeling such mechanical problem were performed throughout the development of the research work [29]. Namely, the approaches included 3D bricks, shells and also beam elements. These approaches differed in various degrees of computational cost, accuracy, collected data and ease of modeling. Finally, the chosen numerical model was the simplest and less expensive computationally. The chosen model provided a reasonably high level of accuracy when balanced with the amount of collected data, the computational cost, and the usefulness of the results obtained for control and monitoring purposes of incrementally launched steel bridges. Other models (including shells) are under further development and may eventually be useful for monitoring instability-related problems during launching.

The steel plate was modeled with first-order beam elements. The rollers and supports were modeled as analytical, rigid and frictionless surfaces on which the steel plate was able to slide and/or transmit contact stresses but conversely, was not able to penetrate through. These analytical surfaces were geometrically defined as semicircular objects rigidly connected to the ground. Mathematically, this contact problem is commonly referred to as the penalty-based method. Further mathematical background behind this procedure is available in [29] and in the Software manuals [31]. A convergence analysis by comparing theoretical and experimental values to the numerically obtained ones was also performed. The beam model proved relatively low mesh-dependent. Table 3 shows the principal characteristics of the model, which is simple and straightforward.

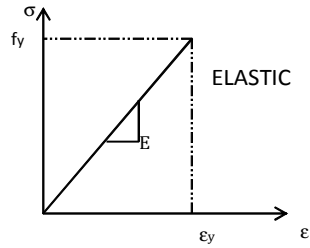
Numerical simulation	
Software	Abaqus
Solver	Abaqus-Standard
Cross-section	60 mm x 4 mm
Material	Steel
E (N/mm ²)	210000
Density (Kg/m ³)	7850
Constitutive equation (Elastic)	
Procedure	Geometrically nonlinear
Contact-Friction	Penalty-based contact.
Interaction	Tangentially: Frictionless Normally: No penetration but separation
Load type	Self-weight
Beam element	B21 first-order, planar
L _{span, scale-reduced} (mm)	2000
Mesh	Uniform. Length= L _{beam} /200
Bearings	Semi-circular rigid wires

Table 3. Characteristics of the numerical model (see Abaqus manuals [29][31])

Fig. 10 displays a lateral view of the numerical reproduction of the scale-reduced test. The point 1 is located precisely at the same position than the strain gauges bonded in the steel plate. Consequently, the strain measurements could be compared. The point 2 is located at the beginning of the launching nose and the displacement results (vertical) were compared to those

measured at the lab. The numerical model includes thus, a steel plate, 11 rollers as well as the central and end bearings (of the same numerical nature than the rollers).

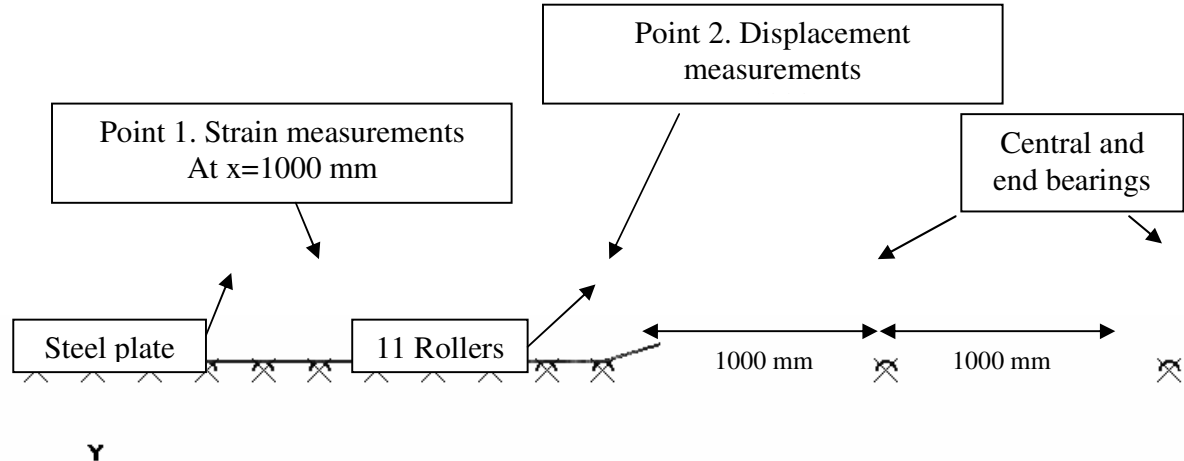


Figure 10. Numerical reproduction of the scale-reduced test. Lateral view.

4.2 Validation of the numerical model

The numerical model was validated by reproducing precisely the experimental test depicted in section 3. The experimentally collected data related to strain and vertical displacements was used as a benchmark. The numerical model including the characteristics depicted in Table 3 provided similar results related to strain and vertical displacement as the steel plate was numerically launched. Fig. 11 displays the comparison between the experimental and the numerical results related to the longitudinal strain of the steel plate at the depicted point 1. Both curves practically coincide (stepwise nature of the experimental results aside). The numerical model reproduces quite satisfactorily the response observed experimentally both qualitatively and quantitatively. A

slight difference between the maximum strain values at both monitored peaks is observable. This difference is attributed to the greater flexibility of the experimental test (Fig. 8)

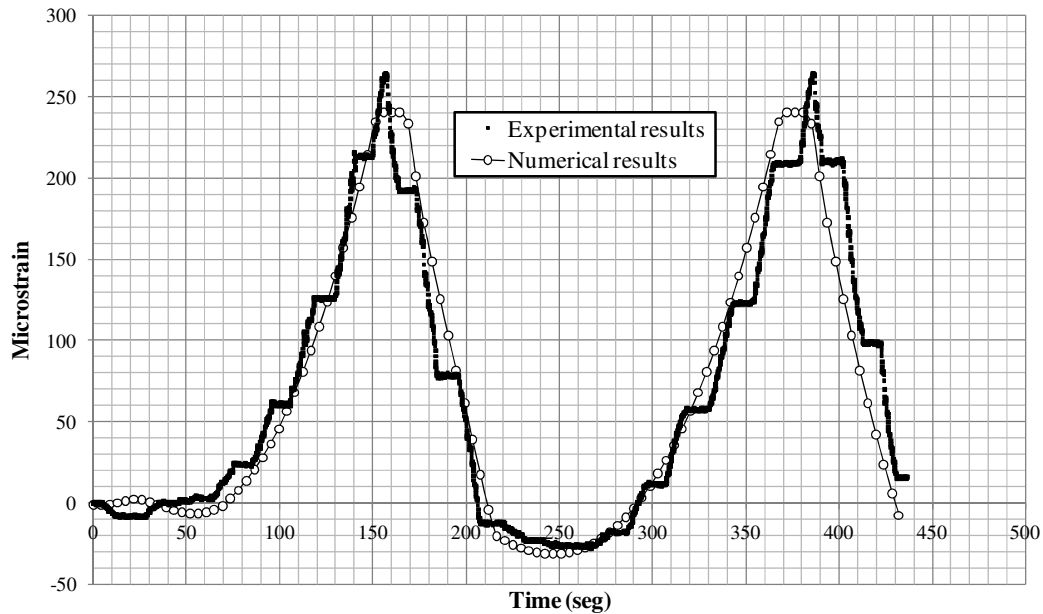


Figure 11. Numerical vs. experimental results related to longitudinal strain

Fig. 12 displays a comparison between the experimental and the numerical results related to the vertical displacement of the steel plate at the depicted point 2. Both curves practically coincide qualitatively but there is a difference in quantitative terms when compared to the strain results at peak points. The differences are, however, rather small. The numerical model yields a slightly more flexible response than the experimental data.

The main novel feature of the numerical model, which is the contact-based formulation between the rollers and the girders, is adequately reproduced.

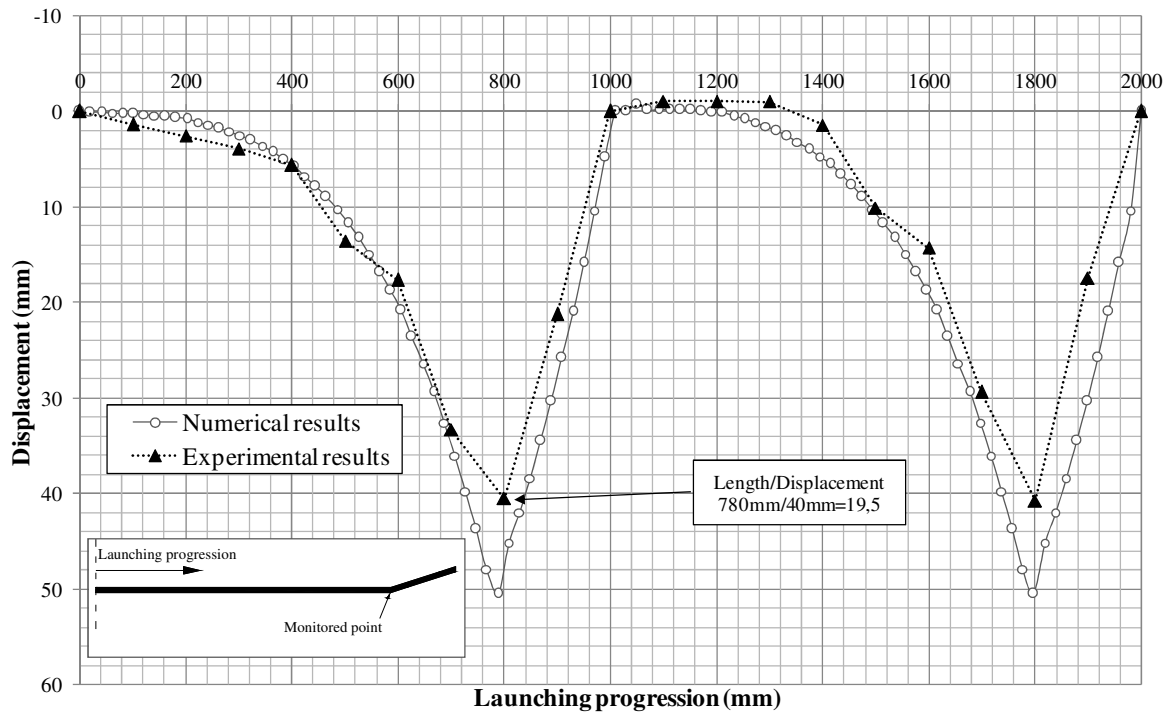


Figure 12. Numerical VS experimental-Vertical displacement.

5. Numerical reproduction of a real scale incrementally launched bridge

A numerical reproduction of a hypothetical ILM of the steel bridge depicted in Fig. 2 was performed with the validated model. The numerical characteristics of such model are identical to those depicted in Table 3. There is, though, a difference worth mentioning: the bearings in this model were created according to the standard dimensions for these devices [23]. These elements were equally modeled as analytical, rigid surfaces. In this case, a regular mesh of 186 first-order beam elements (B21, whose length equals approximately the relationship $L_{\text{span}}/200$) was

348 deployed. The configuration of the launched structure is identical to the one depicted in Fig. 10
349 but in this case, $L=75000$ mm.

350 The numerical model allows the user to extract any kind of information related to the stress,
351 strain, displacement and the contact forces fields. This represents a vast amount of data, which is
352 not necessarily useful during the construction stages. In field bridge engineering, it might be of
353 great usefulness to accurately anticipate the forces, strains and displacements the girder
354 undergoes during the incremental launching procedure. Consequently, the results that are
355 displayed herein are aimed at showing the potential control tools such simulation may provide.
356 Therefore, three structural results are monitored and depicted:

- 357 • Strains at point A (exact middle point of the girder).
- 358 • Vertical displacement at the front of the cantilever
- 359 • Reaction forces at central and end bearings.

360 The abovementioned magnitudes are usually monitored during the launching phase. A thorough
361 comparison between the anticipated values and the field measurements may clarify and/or
362 confirm the correct practice of the launching process or potentially, may prevent undesired
363 problems during construction.

366 5.1 Strains

367 The results concerning stresses and strains are useful in a twofold fashion:

- For design purposes, the model may warn about any potential yielding of the girder during the ILM if the strain is associated with the constitutive equation of the material.

- For control purposes, the results related to strains may be compared with in situ measurements that are increasingly used nowadays [20-23].

For the former, localized yielding of the steel girders during launching is highly undesired. The numerical model provides information that may anticipate any potential yielding of the girder at any point. The numerical model may flag any finite element that overpasses a defined threshold of stresses (namely, the yield stress f_y). The yielded areas could be pinpointed at the end of the procedure and the design of the steel girder may be changed at design stages.

For the latter, the model allows to track the strain at any given point of interest (that may be the points at which strain gauges are located). The stress levels may also be inferred from the strain field via the constitutive equation (which is reasonably expected to be linear during construction).

Fig. 13 displays a control plot of strain and stresses obtained with the numerical simulation of the ILM. The strain-stress values are obtained from point A, which is located where the maximum longitudinal stress occurs.

Noticeably, sign reversals are observable since the girder undergoes consecutive sagging and hogging bending moments. This information should reasonably coincide with the field measurements. Finally, the plot includes thresholds that define warning areas of undesired levels of stress and strain (pinpointed qualitatively in the plot).

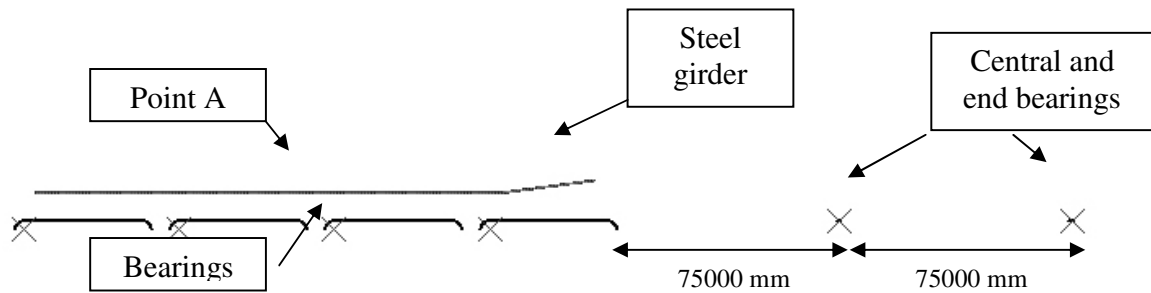


Fig 13. Numerical reproduction of the ILM

5.2 Vertical displacements

The vertical displacements of the steel girders are generally monitored and controlled in situ with basic topographic equipment. These measurements do not require complex acquisition data systems despite the high level of accuracy provided by modern total stations. The contractors, designers and bridge owners often rely on such measurements due to their adequate balance between accuracy and ease. Any individual involved in the construction can track the progression of the launching in terms of deflection of the steel girder.

Fig. 14 displays the history of the vertical displacement of the point referred to as B in the plot obtained with the numerical model. This history should be read as follows, for a given distance x (mm) of the tracked point during launching, its vertical displacement is given. Noticeably, the displacement increases in sagging zones and decreases as the girder passes over a given bearing.

Field measurements and numerical predictions may also be compared and thus, conclusions related to the process may be drawn.

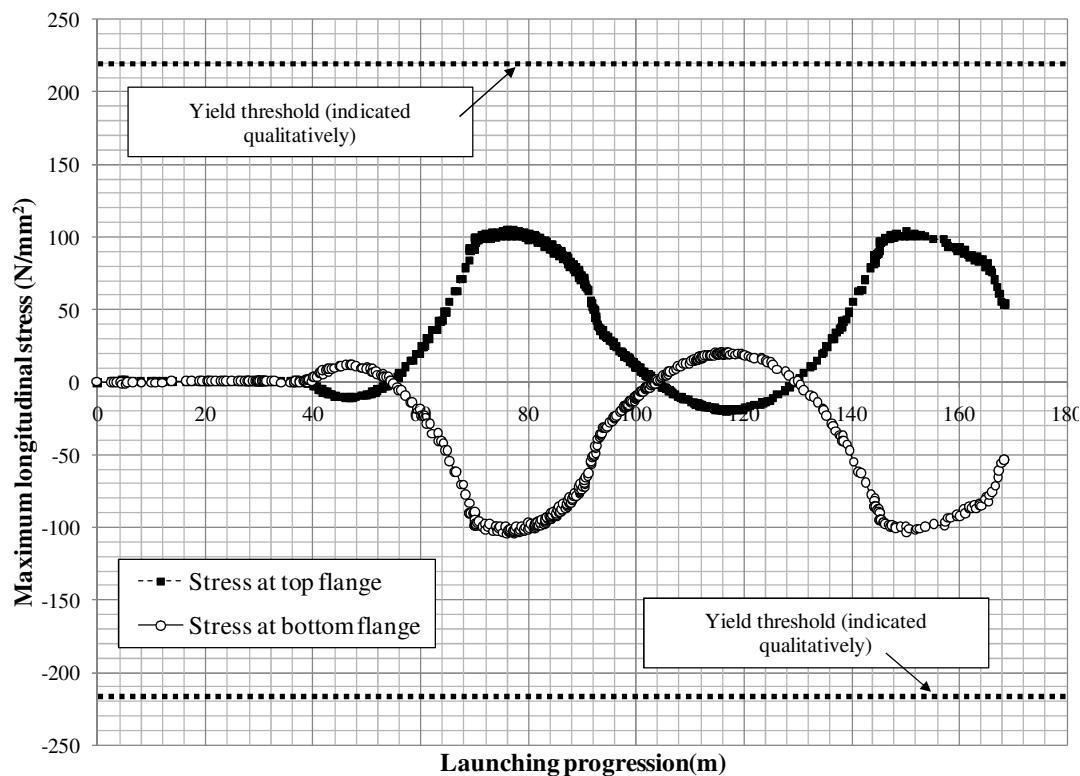


Figure 14. Longitudinal stress control at point A.

5.3 Reaction force at the bearings

Load cells are usually deployed at bearing during launching [32]. These measurements allow to monitor the magnitude of the reaction forces. In bridges with multi-girder cross-sections, these measurements are of the utmost importance for the verification of the adequate position of the bridge during launching. All load cells provided at a given bearing should read a proportional amount of the total load which is known beforehand. If an undesired loss of symmetry occurs

during launching, the reactions forces would differ considerably from one girder to another. This implies repositioning of the bridge with all costs and time-waste associated. .

The numerical model provides information related to the contact stresses transmitted from the girders to the bearing. In addition, it provides information related to the internal forces that occur at the girder (bending moment, shear). Fig. 15 displays a reaction force graph plotted against the distance at which the launching nose is located (namely, the launching progression). The results might be compared with in situ measurements for control purposes but also, these results might be used at design stages. In steel launched bridges, it is well-known that the patch loading forces combined with the bending moments are, among others, important forces to be verified.

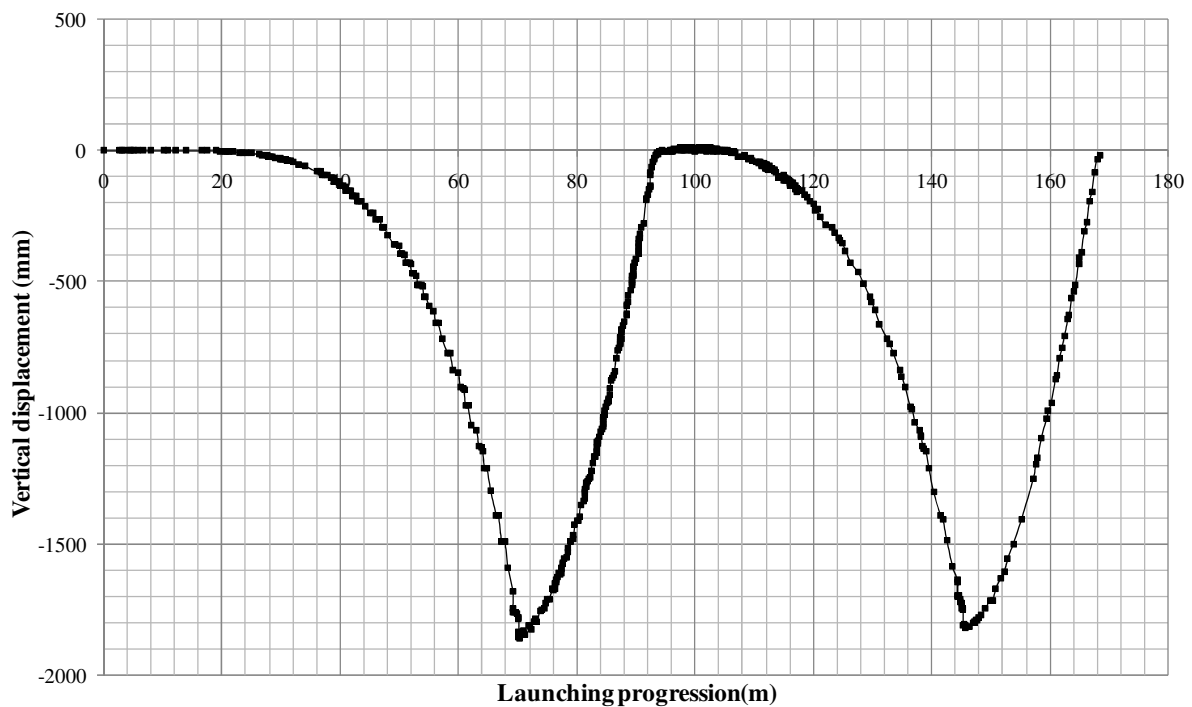


Figure 15. Vertical displacement control of a real-scale launched steel bridge.

Figure 15. Vertical reaction control at central pier and end abutment.

6. Conclusions

In this paper, experimental and numerical models aimed at simulating the structural behavior of a steel I-girder bridge constructed by the incremental launching method (ILM) are depicted.

On the one hand, the experimental test has been performed in a scale-reduced fashion and has been useful for validation purposes. On the other hand, the numerical model using beam elements proves versatile when simulating the launching process within a short calculation time. The numerical model includes a contact-based formulation which reproduces satisfactorily the transient support conditions that occur during the ILM.

The numerical simulation of the ILM represents a useful tool for monitoring and controlling the various magnitudes that are typically measured in situ with traditional field equipment. This numerical control allows bridge designers, contractors and owners to anticipate the structural response of the steel girders. Results related to the strain-stress field, vertical displacements and reaction forces at bearings might be easily inferred from the simulation and compared to field measurements. The proposed simulation of the ILM model provides an adequate balance between accuracy, collected data and ease. The simulation presented herein might be extended to box girders or other bespoke cross-sections.

7. References

[1] LaViolette M., Wipf T., Lee Y. Bridge construction practices using incremental launching, American Association of State Highway and Transportation Officials, AASHTO, 2007.

453

454 [2] Rosignoli M. Bridge Launching, Thomas Telford, 2002.

455

456 [3] Baur W., Bridge Erection by Launching is Fast, Safe and Efficient, Civil Engineering –
457 ASCE, Vol. 47 (3), 1977.

458

459 [4] Gohler B. Pearson P., Incrementally Launched Bridges. Design and Construction,
460 Ernst and Sohn, Berlin, Germany, 2000.

461

462 [5] Alistair P., Large and Small Incrementally Launched Structures, Transportation Research
463 Record 1696 (5B0060), Transportation Research Board, Washington D.C., 2000.

464

465 [6] Zellner, W. and Svensson, H. . Incremental Launching of Structures. Journal of Structural
466 Engineering. Vol 109 (2), 520–537. 1983

467

468

469 [7] Rosignoli M., Site Restrictions Challenge Bridge Design, Concrete International, Vol. 20 (8),
470 1998.

471

472 [8] Rosignoli M. Pre-sizing of Prestressed Concrete Launched Bridges. ACI Structural Journal.
473 Vol. 96 (5), pp. 705-711, 1999.

474

475 [9] Rosignoli M. Nose-Deck Interaction in Launched Prestressed Concrete Bridges. Journal of

476 Bridge Engineering, Vol 3 (1) pp. 21-27. 1998.

477

478 [10] Rosignoli M. Reduced-Transfer-Matrix Method of Analysis of Launched Bridges. ACI
479 Structural Journal, Vol. 96 (4). pp. 603-608. 1999.

480

481 [11] Rosignoli M., Monolithic Launch of the Reggiolo Overpass, Concrete International, Vol. 29
482 (2), 2001.

483

484 [12] Granath P., Distribution of support reaction against a steel girder on a launching shoe,
485 Journal of Constructional Steel Research, Vol 47 (3), pp. 245-270. 1998

486

487 [13] Granath P., Thorsson A., Edlund B., I-shaped steel girders subjected to bending moment and
488 travelling patch loading, Journal of Constructional Steel Research, Vol 54 (3), pp. 409-421. 2000

489

490 [14] Granath P., Serviceability limit state of I-shaped steel girders subjected to patch loading,
491 Journal of Constructional Steel Research, Vol. 54 (3), pp. 387-408. 2000

492

493 [15] Favre R., Badoux M., Burdet O., Laurencet P., Incremental Launching for the Ile Falcon
494 Bridge, Concrete International, Vol. 21 (2), February 1999.

495

496 [16] Hewson N., Hodgkinson A., Incremental Launch of Brides Glen Bridge, Ireland,
497 Concrete, Vol. 38 (7), 2004

498

499 [17] Zhuravov L., Chemerinsky O., Seliverstov V., Launching Steel Bridges in Russia, Journal
500 of International Association for Bridge and Structural Engineering (IABSE), Vol. 6 (3), pp. 183-
501 186. 1996
502

503 [18] Marzouk M., El-Dein H., El-Said M., Application of computer simulation to construction of
504 incrementally launching bridges, Journal of Civil Engineering and Management, Vol. 13 (1), pp:
505 27-36. 2007
506

507 [19] Rongqiao X, Binlei Shao. A new beam element for incremental launching of bridges,
508 Journal of Bridge Engineering, pp: 1-19. 2011
509

510 [20] Chacón R., Guzmán F., Mirambell E., Real E., Oñate E. Wireless Sensor Networks for
511 strain monitoring during steel bridges launching, International Journal of Structural Health
512 Monitoring, Vol 8 (3), pp: 195-205, 2009
513
514

515 [21] Wipf T., Phares B., Abendroth R., Chang B., Abraham S., Monitoring of the
516 Launched Girder Bridge over the Iowa River on US 20, Final Report CTRE Project 01-108,
517 Center for Transportation Research and Education, Iowa State University. March 2004.
518

519 [22] Lebet J. Measurements taken during the launch of the 130 m Span Vaux Viaduct,
520 Steelbridge, OTUA. Millau, France. (2004)

[23] Zhang Y., Luo R. Patch loading and improved measures of incremental launching of steel box girder. Journal of Constructional Steel Research. Vol 68 (1), pp:11-19. 2012

[24] Martins O.P., Sampaio A.Z., Bridge launching construction visualized in a virtual environment. The International Journal of Virtual Reality. Vol. 10 (2), pp: 49-56. 2011.

[25] Combri Design Manual –Part I Applications of Euro Code rules, first edition, 2008.

[26] Buckingham E., On physically similar systems. Illustrations of the use of dimensional equations. Physical Review, Vol. 4, pp: 345-376. 1914.

[27] Blanco E., Oller S., Gill L. Análisis Experimental de estructuras, CIMNE, Barcelona, Spain, 2007 (in spanish)

[28] CATMAN Easy V 6.10. Hottinger Baldwin Messtechnik HBM 2012.

[29] Uribe N., Reproducción numérica y experimental del proceso de lanzamiento de un puente metálico por empujes sucesivos. Master's Thesis. Construction Engineering Department.

ETSICCPB. Universitat Politècnica de Catalunya. 2012 (in spanish)

<http://upcommons.upc.edu/pfc/handle/2099.1/14898>

[30] Lindgren B.W., Statistical theory 2nd Edition, The Mcmillan Company, New York, 1962.

544 [31] Abaqus FEA, Simulia© V6.10.3. Dassault Systèmes. 2012.

545

546 [32] Marzouk M., Said H., El-Said M., Framework for multiobjective optimization of launching
547 girder bridges. Journal of Construction Engineering and Management. Vol 135 (8), pp 791-800.

548 2011